

An aeroacoustic mechanism to explain universal behavior in hypersonic wake flow oscillations

Premika S. Thasu,* Gaurav Kumar,† and Subrahmanyam Duvvuri‡

*Turbulent Shear Flow Physics and Engineering Laboratory
Department of Aerospace Engineering, Indian Institute of Science, Bengaluru 560012, India*

(Dated: July 10, 2024)

Recent experimental studies reveal that the near-wake region of a circular cylinder at hypersonic Mach numbers exhibits self-sustained flow oscillations. The oscillation frequency was found to have a universal behavior. Experimental observations suggest an aeroacoustic feedback loop to be the driving mechanism of oscillations. An analytical aeroacoustic model which predicts the experimentally observed frequencies and explains the universal behavior is presented here. The model provides physical insights and informs of flow regimes where deviations from universal behavior are to be expected.

The wake of a 2D circular cylinder in the incompressible flow regime is a celebrated canonical problem in fluid dynamics [1–3]. Historically, the cylinder wake problem was at the forefront of research in fluid dynamics, with motivation coming partly from practical issues in understanding and predicting hydrodynamic drag force on bluff bodies [2–4]. The canonical cylinder wake contains many of the key elements of a generic bluff body wake. In the incompressible flow regime the physics of the wake is governed by a single non-dimensional parameter: the Reynolds number $Re_D = (\rho_\infty U_\infty D)/\mu_\infty$. Here U_∞ is the freestream flow velocity, D is the cylinder diameter, and ρ_∞ and μ_∞ are the density and dynamic viscosity, respectively, of the freestream fluid.

Periodic vortex shedding from the aftbody of the cylinder, which is a commonly observed flow feature in incompressible cylinder wakes, gives the flow a visually appealing character. (This is popularly known as the *Kármán vortex street*; see Fig. 1a.) As Re_D is increased starting from $Re_D \ll 1$, the phenomenon of vortex shedding manifests at $Re \approx 47$ [5]. Vortex shedding gives the wake a characteristic timescale, which is written in the form of a non-dimensional frequency referred to as the Strouhal number $St = (fL)/U$. Here f is the characteristic frequency of flow oscillations in the wake region, and L and U are characteristic length and velocity scales, respectively. It is noted that St is a function of Re_D . An interesting and fundamentally important aspect of St is its universal behavior; when the shedding frequency is scaled using the wake width and a characteristic wake velocity, St attains invariance for $Re_D > 300$, with a value of approximately 0.164 [3, 6–9]. This universal behaviour holds across a broad range of Reynolds numbers for cylinders and also for other bluff body shapes in the incompressible flow regime [9–11].

Relaxing the incompressibility condition presents a more general problem of the wake flow in the compressible regime, where the Mach number becomes an additional (and independent) governing parameter along with the Reynolds number. The freestream flow Mach number is defined as $M_\infty = U_\infty/a_\infty$, where a_∞ is the acoustic wave speed. The 2D cylinder wake at supersonic and hypersonic Mach numbers, where the flow is compressible, is very distinct from its incompressible flow regime counterpart. As a representative example, Fig. 1b shows an instantaneous flow density gradient map for a cylinder at $M_\infty = 6$. Distinction between incompressible and compressible cylinder wake flows are qualitatively very evident in Fig. 1. For $M_\infty > 1$, shock waves appear in the flow and the vortex shedding phenomenon disappears. The near-wake region is characterized by the formation of two shear layers, which are symmetric about the cylinder centerline.

The canonical compressible cylinder wake problem has received much less scientific attention as compared to the incompressible problem. The near-wake periodic flow unsteadiness in the incompressible regime has been the subject of several detailed studies [2, 3], which span a period of over a hundred years [12], and the unsteadiness mechanisms are reasonably well understood [3, 13–15]. Whereas for the supersonic/hypersonic flow regime, it is only within the past decade that the near-wake flow region was discovered to exhibit coherent and periodic oscillations [16–18] [19]. The oscillations were found to have a single characteristic frequency. Interestingly, the oscillation Strouhal number, formed using the shear layer length and freestream velocity, exhibits universal behavior. At high-supersonic and hypersonic Mach numbers and across a range of Reynolds numbers, the Strouhal number was found to be invariant, taking a value of approximately 0.48 [16, 17].

The nature of cylinder wake unsteadiness in the compressible flow regime is fundamentally very different from the incompressible flow scenario. Driven by experimental observations, literature proposes the following hy-

* Email address: premikat@iisc.ac.in

† presently at the University of Nevada, Reno

‡ Corresponding author; email address: subrahmanyam@iisc.ac.in

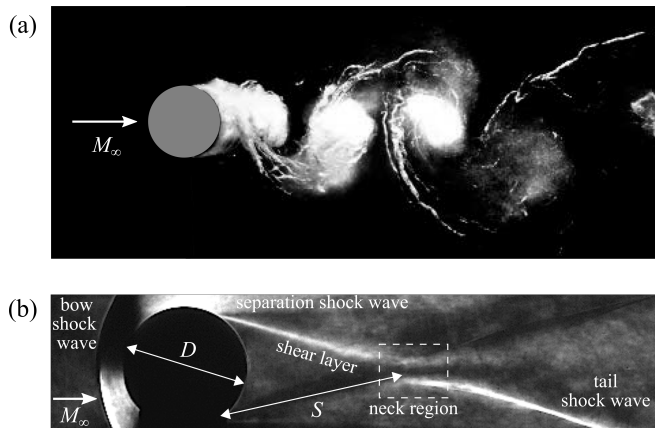


FIG. 1: (a) An instantaneous snapshot of cylinder wake flow in water at $M_\infty = 0.01$ and $Re_D = 1.4 \times 10^5$ [20]. The shedding vortices from the top and bottom of the cylinder aftbody, with opposing sense of rotation, are visualized by controlled cavitation [20]. (b) An instantaneous density gradient map around a circular cylinder at $M_\infty = 6$ and $Re_D = 2.8 \times 10^5$ obtained using the optical imaging technique of schlieren [17].

pothesis: an aeroacoustic feedback mechanism in the near-wake causes and sustains flow oscillations [16, 17]. Based on this hypothesis, here we develop a quantitative aeroacoustic model with no empiricism to explain oscillations observed in the supersonic/hypersonic cylinder wake. The model successfully predicts the oscillation frequencies reported from experiments, and thereby provides a clear physical understanding of the phenomenon. Further, the model also explains the experimentally observed universal behavior and informs of flow regimes where deviations from universal behavior are to be expected. Table I summarizes the experimental data available in literature for near-wake oscillations at high Mach numbers. S is the shear layer length (see Fig. 1b), and two Strouhal numbers are defined as $St_D = (fD)/U_\infty$ and $St_S = (fS)/U_\infty$. Data from Table I are used for the present model development exercise and for validation of model predictions.

We begin with a brief description of the key flow features (see Fig. 2). Given the flow symmetry about the cylinder centerline, only the top half of the cylinder and flow are depicted in the figure. A steady bow shock wave forms upstream of the cylinder, and the flow downstream of the shock wave in region 2 is subsonic. The subsonic fluid accelerates as it moves around the cylinder, attains Mach 1 at the sonic line, and further accelerates to supersonic Mach numbers as the flow expands around the cylinder. Further downstream the flow separates from the cylinder surface (due to the limitation on the maximum turn angle of supersonic flows) and generates a separation shock wave. Flow separation on the top and bottom surfaces of the cylinder results in the formation

	M_∞	$Re_D (\times 10^4)$	$\frac{S}{D}$	St_D	St_S
Schmidt and Shepherd [16]	4	2	1.52	0.299	0.45
		4	1.84	0.308	0.56
		5	1.23	0.339	0.42
		9	1.28	0.368	0.47
		13	1.35	0.398	0.53
		21	1.27	0.459	0.58
Thasu and Duvvuri [17]	6	23	1.49	0.341	0.5
		28	1.39	0.346	0.48
		30	1.38	0.349	0.48
		40	1.38	0.355	0.49
		43	1.3	0.361	0.47
		50	1.27	0.372	0.47

TABLE I: Strouhal number data from experiments.

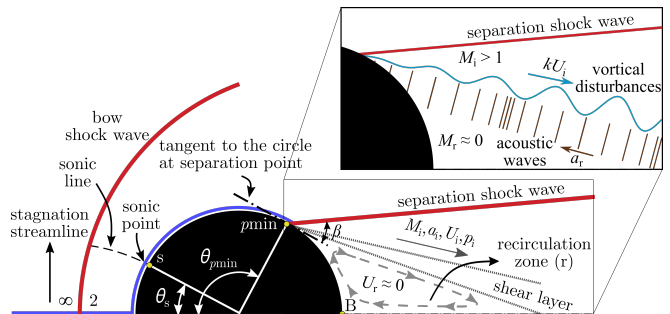


FIG. 2: A schematic illustration of the flow structure over the top half of a supersonic/hypersonic cylinder.

of symmetric supersonic shear layers on either side of the centerline. The region of intersection of the two shear layers is referred to as the “neck” of the wake (marked in Fig. 1b). The shear layers and the cylinder surface enclose two regions of subsonic recirculating flow with opposing sense of rotation. Downstream of the neck the flow turns parallel to the freestream through tail shock waves that are generated at the neck region.

The physical picture of flow oscillations that we build on is the following: interaction between the two shear layers in the neck region leads to an aeroacoustic feedback loop and sustains periodic flow oscillations. The inset in Fig. 2 illustrates this mechanism, which comprises of four distinct phases:

1. downstream propagation and amplification of vortical disturbances (generated by flow instabilities) in the shear layers;
2. scattering, or generation of acoustic disturbances, at the neck region due to interaction between the two unsteady shear layers;

3. upstream propagation of acoustic waves along the subsonic portion of the shear layers;
4. receptivity of the shear layers to the acoustic waves, resulting in the excitation of vortical disturbances in their upstream regions.

It is noted that a broadly similar mechanism to the one outlined above is at play when air flows at high subsonic or supersonic speeds over open cavities, and leads to periodic unsteadiness and emission of acoustic tones. Some insights from open cavity flow literature, particularly the modeling framework used therein [21–23], are leveraged for the present effort.

By considering the feedback loop to be linear, and matching the wavespeed to wavelength ratio (*i.e.*, frequency) between downstream-propagating vortical disturbances and upstream-propagating acoustic disturbances, the following expression can be obtained for the disturbance frequency f [21–23]:

$$f = \left(\frac{1}{S}\right) \left(\frac{m - \phi}{\frac{1}{a_r} + \frac{1}{kU_i}}\right). \quad (1)$$

Here U_i is the flow velocity downstream of the separation shock wave (see Fig. 2), kU_i is the propagation speed of vortical disturbances (with k being a constant), a_r is the speed of the acoustic waves that propagate upstream along the shear layer of length S , integer m is the mode number for the oscillations, and ϕ is the phase difference between the vortical and acoustic disturbances at the neck region. The flow oscillation timescale is taken to be the same as the vortical and acoustic disturbance timescale, *i.e.*, f also denotes the wake oscillation frequency. The Strouhal number St_D of wake oscillations can then be written as

$$St_D = \frac{fD}{U_\infty} = \left(\frac{D}{S}\right) \left(\frac{m - \phi}{\frac{U_\infty}{a_r} + \frac{U_\infty}{kU_i}}\right). \quad (2)$$

Obtaining the exact conditions downstream of the separation shock waves requires detailed flow computations. However, with certain simplifications, the flow conditions can be estimated reasonably well without resorting to computations. An acceptable modeling approximation is to consider flow along the stagnation streamline (marked in Fig. 2) downstream of the bow shock wave to be isentropic. Flow stagnation properties downstream of the bow shock wave (region 2 in Fig. 2) are obtained by assuming the bow shock wave to be locally normal in the region close to the cylinder centerline [24]. The pressure minimum location on the cylinder surface, marked as $\theta_{p\min}$ in Fig. 2, occurs slightly upstream of the region where the separation shock wave forms [25]. Flow properties at $\theta_{p\min}$ are obtained using the Prandtl-Meyer expansion fan theory [24] with the flow turn angle given by the difference in angle between $\theta_{p\min}$ [25] and the sonic point location θ_s [26]. The solution of the separation shock

wave requires information on at least one flow property downstream. From earlier studies of compressible cylinder wake flows aimed at understanding the mean (time-averaged) flow structure [25, 27–29], the base pressure ratio is consistently observed to be $p_B/p_{02} = 0.03 \pm 0.01$, where p_B denotes the pressure at the base of the cylinder (denoted as ‘B’ in Fig. 2), and p_{02} represents the pressure at the forward stagnation point. Measurements from recent experiments at Mach 6 show a pressure ratio $p_B/p_{02} = 0.025$ [30], which is in good agreement with earlier literature. Since significant pressure gradients are not expected in the recirculation region, the pressure downstream of the separation shock wave (p_i) is taken to be $p_i = p_B$. By using the flow properties at the pressure minimum location as the upstream conditions and p_i as the downstream condition, a solution for the separation shock wave angle (β) and strength can be obtained using standard oblique shock wave relations [24].

In the recirculation region the flow velocities are relatively very low, and hence the region is regarded as stagnant. The acoustic speed in this region, denoted as a_r , is estimated by determining the average local temperature T_r within the recirculation region. The recovery temperature is a good estimate for T_r since it accounts for viscous losses in the shear layer [31, 32]. The recovery temperature is given by

$$T_r = \left[\frac{1 + \sqrt{Pr} \left(\frac{\gamma-1}{2}\right) M_i^2}{1 + \left(\frac{\gamma-1}{2}\right) M_i^2} \right] T_0, \quad (3)$$

where T_0 is the stagnation temperature, Pr is the Prandtl number, γ is the ratio of specific heats for the fluid, and M_i is the Mach number downstream of the separation shock wave. With R as the gas constant, a_r is then written as

$$a_r = \sqrt{\gamma RT_r}. \quad (4)$$

The propagation speed of the vortical disturbances (kU_i) is estimated by modeling the compressible shear layer as a 2D mixing layer, with supersonic flow on the top and stagnant fluid on the bottom. Extensive literature is available on compressible mixing layers, including studies on growth rate of shear layer thickness and the convection speed of disturbances [33–38]. Flow instabilities in mixing layers consist of three families of waves, labeled as “Kelvin-Helmholtz,” “supersonic,” and “subsonic” instability waves [39–41]. Propagation speeds of these waves can formally be obtained through linear stability analysis of the mixing layer [39]. For the present purpose, however, a simple vortex train model of these instability waves [42] is used to obtain reasonably accurate estimates for the propagation speeds. The vortex train model gives the propagation (or convection) speeds w_{sup} , w_{KH} , w_{sub} of supersonic, Kelvin-Helmholtz, sub-

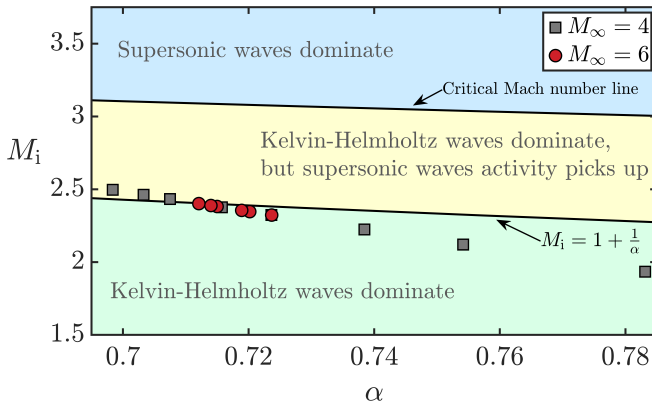


FIG. 3: A map of dominant instability waves in the $[M_i, \alpha]$ parameter space. Square and circle markers correspond to experimental data given in Table I.

sonic instability waves, respectively, as

$$\begin{aligned} \frac{w_{\text{sup}}}{U_i} &= \frac{1}{1 + \alpha} \\ \frac{w_{\text{KH}}}{U_i} &= \frac{1 + \alpha \left(\frac{w_{\text{sup}}}{U_i} \right)}{1 + \alpha} = \frac{1 + 2\alpha}{(1 + \alpha)^2} \\ \frac{w_{\text{sub}}}{U_i} &= \frac{1 - \alpha \left(\frac{w_{\text{sup}}}{U_i} \right)}{1 + \alpha} = \frac{1}{(1 + \alpha)^2}. \end{aligned} \quad (5)$$

Here $\alpha = a_i/a_r$ is the ratio of sound speeds between the supersonic flow side and the stagnant flow side of the shear layer (see Fig. 2). It is noted that all three non-dimensional propagation speeds (w_{sup}/U_i , w_{KH}/U_i , w_{sub}/U_i) are solely a function of α .

Based on harmonic analysis of linearized governing equations of compressible inviscid mixing layer flow [39], some key observations of the instability wave characteristics are made here. At low supersonic Mach numbers, only the Kelvin-Helmholtz and subsonic instability waves are active, with the Kelvin-Helmholtz waves dominating the flow. Supersonic instability waves emerge only when $M_i > 1 + (1/\alpha)$ [39]. The growth rates of Kelvin-Helmholtz and supersonic instability waves depend on M_i and α . Specifically, as M_i increases, the dominance of Kelvin-Helmholtz instability waves decreases while the growth rate of supersonic instability waves steadily rises. The Mach number M_i above which supersonic instabilities become dominant is termed the critical Mach number. Subsonic waves are active only when the mixing layer has a finite (but small) thickness. Their growth rates are small, and hence they are considered to be the least unstable of the three wave families [39]. Fig. 3 shows a map of the $[M_i, \alpha]$ parameter space, wherein the M_i and α values for the experimental data points given in Table I are estimated using the modeling approach outlined earlier in this paper. The figure clearly shows that Kelvin-Helmholtz instability waves are expected to be

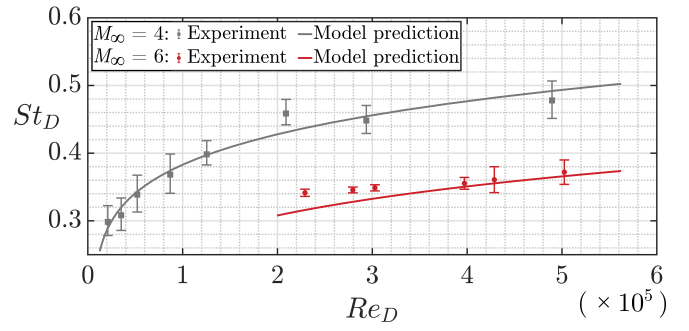


FIG. 4: Strouhal number comparison between experimental data and predictions from present model.

the dominant instability waves in the wake shear layers across all the experimental data points considered here. Hence, the propagation velocity of vortical disturbances (kU_i) in Eqns. (1) and (2) is taken to be the convection velocity of the Kelvin-Helmholtz instability waves w_{KH} (Eq. 5); we have

$$kU_i = w_{\text{KH}} = \frac{1 + 2\alpha}{(1 + \alpha)^2} U_i. \quad (6)$$

The shear layer length S for use in Eq. (2) is obtained from experimental data given in Table I. The mode number in Eq. (2) is taken as $m = 2$ [43]. Based on open cavity flow observations [44], the value of ϕ is set to 0.25, which corresponds to a phase difference of 90° between the acoustic and the vortical disturbances at the neck. With that, the modeling exercise is complete, and St_D can be predicted using Eq. (2). The Strouhal number predictions from the model are compared against experimental data in Fig. 4. The model is seen to perform well in predicting the experimental measurements at both $M_\infty = 4$ and 6. Hence, this exercise lends clear support to the hypothesis that the aeroacoustic mechanism outlined here drives the near-wake oscillations.

We now consider St_S :

$$St_S = St_D \left(\frac{S}{D} \right) = \frac{m - \phi}{\frac{U_\infty}{a_r} + \frac{U_\infty}{kU_i}}. \quad (7)$$

Unlike St_D , St_S does not depend on the geometric parameters S , D . The numerator ($m - \phi$) in the above equation is a constant, and the first and the second terms of the denominator account for the roles of acoustic waves and vortical disturbances, respectively, in the feedback loop. From Eqns. (3), (4), (6), it is seen that the denominator in Eq. 7 depends only on the flow conditions downstream of the separation shock wave (region i) and α , both of which in turn depend on M_∞ and Re_D . Hence we write

$$St_S = g(M_\infty, Re_D), \quad (8)$$

where g indicates functional dependence. The above equation essentially reiterates the fact that the Mach and

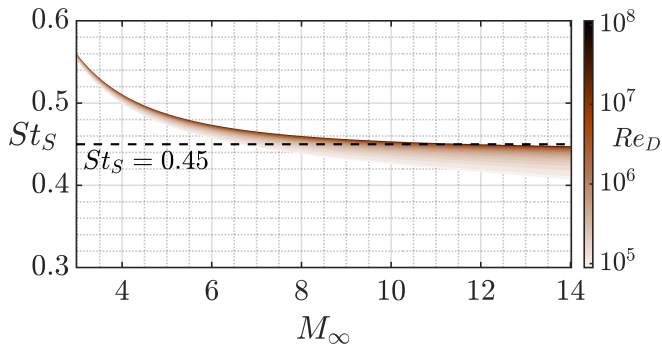


FIG. 5: Model prediction for Strouhal number variation with the two governing parameters, M_∞ and Re_D .

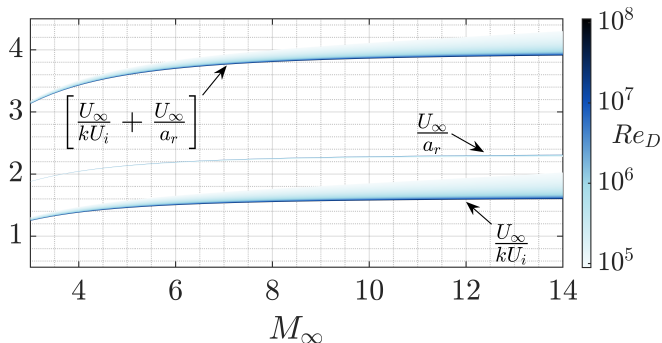


FIG. 6: Variation in propagation speeds of vortical and acoustic disturbances.

Reynolds numbers are the two governing parameters for the cylinder wake in the compressible flow regime. The function g constructed using the aeroacoustic model (*i.e.*, by using Eq. 7) is shown in Fig. 5 [45]. St_S shows a considerable dependence on M_∞ at low values of M_∞ , whereas the dependence becomes increasingly weaker at higher M_∞ . Re_D has a relatively smaller effect, with St_S showing only a small variation across four orders of Re_D . The model predicts that St_S attains an invariant value of 0.45 at large M_∞ and Re_D . Considering the simple nature of the model [46], the prediction is found to be very close to the value of 0.48 reported in literature [16, 17]. Further, the model predicts that the universal behavior breaks at lower supersonic Mach numbers, where St_S is expected to be sensitive to M_∞ .

It is noted that the vortical and acoustic disturbance propagation speeds (kU_i and a_r , respectively) are the velocity scales relevant for the feedback loop. We now consider behavior of these disturbance propagation speeds when scaled by the freestream flow velocity, *i.e.*, the quantities (kU_i/U_∞) and (a_r/U_∞) . Fig. 6 shows the variation of $(kU_i/U_\infty)^{-1}$ and $(a_r/U_\infty)^{-1}$ with M_∞ and Re_D obtained from the model [47]. It is seen that at high Mach and Reynolds numbers, the disturbance propagation speeds scaled by U_∞ become invariant (and thereby the quantity $[U_\infty/a_r + U_\infty/kU_i]$ in Eq. 7 also becomes

invariant). Therefore, U_∞ can be treated as the single relevant velocity scale for the feedback loop. Further, it is noted that the length over which both vortical and acoustic disturbances propagate is S , which naturally makes it the relevant length scale for oscillations. From these arguments we conclude that U_∞ and S are the appropriate velocity and length scales, respectively, to form the Strouhal number (*i.e.*, St_S). And, when the oscillation frequency f is scaled with S and U_∞ , we should expect to see invariant behavior at high Mach and Reynolds numbers. This explains the universal behavior of St_S observed in experiments.

- [1] A. Roshko, Experiments on the flow past a circular cylinder at very high Reynolds number, *Journal of Fluid Mechanics* **10**, 345 (1961).
- [2] T. Y.-T. Wu, Cavity and wake flows, *Annual Review of Fluid Mechanics* **4**, 243 (1972).
- [3] C. H. K. Williamson, Vortex dynamics in the cylinder wake, *Annual Review of Fluid Mechanics* **28**, 477 (1996).
- [4] A. Roshko, Perspectives on bluff body aerodynamics, *Journal of Wind Engineering and Industrial Aerodynamics* **49**, 79 (1993).
- [5] C. P. Jackson, A finite-element study of the onset of vortex shedding in flow past variously shaped bodies, *Journal of Fluid Mechanics* **182**, 23 (1987).
- [6] A. Roshko, *On the Development of Turbulent Wakes from Vortex Streets*, Ph.D. thesis, California Institute of Technology (1952).
- [7] A. Roshko, *On the drag and shedding frequency of two-dimensional bluff bodies*, Tech. Rep. 169 (National Advisory Committee for Aeronautics, 1954).
- [8] P. W. Bearman, On vortex street wakes, *Journal of Fluid Mechanics* **28**, 625–641 (1967).
- [9] O. M. Griffin, Universal similarity in the wakes of stationary and vibrating bluff structures, *Journal of Fluids Engineering* **103**, 52 (1981).
- [10] H. B. Awbi, An assessment of the universal strouhal number concepts for two-dimensional bluff bodies, *The Aeronautical Journal* **85**, 467–469 (1981).
- [11] E. Anderson and A. Szewczyk, A look at a universal parameter for 2-D and 3-D bluff body flows, *Journal of Fluids and Structures* **10**, 543 (1996).
- [12] R. N. Govardhan and O. N. Ramesh, A stroll down Kármán street, *Resonance* **10**, 25 (2005).
- [13] F. H. Abernathy and R. E. Kronauer, The formation of vortex streets, *Journal of Fluid Mechanics* **13**, 1–20 (1962).
- [14] J. H. Gerrard, The mechanics of the formation region of vortices behind bluff bodies, *Journal of Fluid Mechanics* **25**, 401–413 (1966).
- [15] A. E. Perry, M. S. Chong, and T. T. Lim, The vortex-shedding process behind two-dimensional bluff bodies, *Journal of Fluid Mechanics* **116**, 77–90 (1982).
- [16] B. E. Schmidt and J. E. Shepherd, Oscillations in cylinder wakes at Mach 4, *Journal of Fluid Mechanics* **785**, R3 (2015).
- [17] P. S. Thasu and S. Duvvuri, Strouhal number universality in high-speed cylinder wake flows, *Physical Review*

- Fluids **7**, L081401 (2022).
- [18] M. Awasthi, S. McCreton, D. J. Moreau, and C. J. Doolan, Supersonic cylinder wake dynamics, *Journal of Fluid Mechanics* **945**, 10.1017/jfm.2022.517 (2022).
- [19] A schlieren video of these flow oscillations is available as supplementary material to reference [17].
- [20] H. Djeridi, M. Braza, R. Perrin, G. Harran, E. Cid, and S. Cazin, Near-wake turbulence properties around a circular cylinder at high reynolds number, *Flow, Turbulence and Combustion* **71**, 19 (2003).
- [21] A. Powell, On edge tones and associated phenomena, *Acta Acustica United with Acustica* **3**, 233 (1953).
- [22] A. Powell, Theory of Vortex Sound, *The Journal of the Acoustical Society of America* **36**, 177 (1964).
- [23] J. E. Rossiter, *Wind-tunnel experiments on the flow over rectangular cavities at subsonic and transonic speeds*, Tech. Rep. 3348 (Aeronautical Research Council Reports & Memoranda, 1964).
- [24] H. W. Liepmann and A. Roshko, *Elements of Gas Dynamics* (New York: John Wiley & Sons., 1957).
- [25] W. S. Hinman and C. T. Johansen, Reynolds and Mach number dependence of hypersonic blunt body laminar near wakes, *AIAA Journal* **55**, 500 (2017).
- [26] J. Sinclair and X. Cuia, A theoretical approximation of the shock standoff distance for supersonic flows around a circular cylinder, *Physics of Fluids* **29**, 10.1063/1.4975983 (2017).
- [27] J. F. McCarthy and T. Kubota, A study of wakes behind a circular cylinder at M equal 5.7, *AIAA Journal* **2**, 629 (1964).
- [28] C. F. Dewey, Near wake of a blunt body at hypersonic speeds, *AIAA Journal* **3**, 1001 (1965).
- [29] G. Park, S. L. Gai, and A. J. Neely, Laminar near wake of a circular cylinder at hypersonic speeds, *AIAA Journal* **48**, 246 (2010).
- [30] P. S. Thasu, *Self-Sustained Oscillations in High-Speed Cylinder Wake Flows*, Ph.D. thesis, Indian Institute of Science (2024).
- [31] J. D. Anderson, *Fundamentals of Aerodynamics*, 6th ed. (McGraw-Hill Education, 1984).
- [32] G. Kumar, V. Sasidharan, A. G. Kumara, and S. Duvvuri, A model for frequency scaling of flow oscillations in high-speed double cones, *Journal of Fluid Mechanics* (accepted for publication), <https://arxiv.org/abs/2401.01538>.
- [33] D. W. Bogdanoff, Compressibility effects in turbulent shear layers, *AIAA Journal* **21**, 926 (1983), <https://doi.org/10.2514/3.60135>.
- [34] D. Papamoschou and A. Roshko, The compressible turbulent shear layer: an experimental study, *Journal of Fluid Mechanics* **197**, 453–477 (1988).
- [35] G. S. Elliott and M. Samimy, Compressibility effects in free shear layers, *Physics of Fluids A: Fluid Dynamics* **2**, 1231 (1990).
- [36] J. L. Hall, P. E. Dimotakis, and H. Rosemann, Experiments in nonreacting compressible shear layers, *AIAA Journal* **31**, 2247 (1993), <https://doi.org/10.2514/3.11922>.
- [37] R. C. Murray and G. S. Elliott, Characteristics of the compressible shear layer over a cavity, *AIAA Journal* **39**, 846 (2001).
- [38] C. Pantano and S. Sarkar, A study of compressibility effects in the high-speed turbulent shear layer using direct simulation, *Journal of Fluid Mechanics* **451**, 329–371 (2002).
- [39] C. K. W. Tam and F. Q. Hu, On the three families of instability waves of high-speed jets, *Journal of Fluid Mechanics* **201**, 447 (1989).
- [40] H. Oertel Sen, Mach wave radiation of hot supersonic jets, in *Mechanics of Sound Generation in Flows* (1979) pp. 275–281.
- [41] H. Oertel Sen, Coherent structures producing mach waves inside and outside of the supersonic jet, in *Structure of Complex Turbulent Shear Flow* (Springer Berlin Heidelberg, 1983) pp. 334–343.
- [42] H. Oertel Sen, F. Seiler, J. Srulijes, and R. Hruschka, Mach waves produced in the supersonic jet mixing layer by shock/vortex interaction, *Shock Waves* **26**, 231 (2016).
- [43] This choice is guided by frequencies observed in experiments [16, 17], which suggest that the second mode frequency is active in the flow.
- [44] D. Rockwell and E. Naudascher, Self-sustained oscillations of impinging free shear layers, *Annual Review of Fluid Mechanics* **11**, 67 (1979).
- [45] For the entire range of M_∞ and Re_D considered here, M_i and α are found to be such that Kelvin-Helmholtz waves are dominant throughout. Hence Eq. (6) is used without any modifications for generating Fig. 5.
- [46] The model neglects the effects of viscosity and non-isentropic behavior of flow around the cylinder forebody.
- [47] Variation is shown for inverse of the scaled propagation speeds since the denominator of Eq. 7 contains inverse of the speeds.